Kenza Djermane, Syham Kadri\*, Abdelhafid Habbab and Elhouaria Bourbaba

# Numerical Investigation of the Cooling Temperature of the InGaP/InGaAs/Ge Subcells Under the Concentrated Illumination

https://doi.org/10.1515/zna-2019-0263 Received August 8, 2019; accepted October 13, 2019; previously published online November 8, 2019

Abstract: The multijunction solar cells performances study is essential for the design of the high-concentration photovoltaic. These cells can operate over a wide range of the incident radiation flux and a large temperature range. These two parameters (concentration and temperature) degrade the cell and require a cooling system. In this article, we have studied numerically the cooling temperature of InGaP/lnGaAs/Ge subcells under the concentrated illumination. For this, we have presented the performance of each subcell as a function of the temperature and concentration sunlight. The different high concentrations ratios (1, 10, 100, and 1000 sun) have been conducted according to the dish-style concentration photovoltaic system for three temperature values T = 300, 500, and 800 K. The results show that under high concentrated light intensity conversion, the performances of these three subcells (efficiency, open-circuit voltage, short-circuit current, and fill factor) were decreased with increasing the temperature. The main objective of this study is to find the limit temperature of each subcell in order to introduce the cooling system. Thus, we can avoid the degradation of the tandem solar cell under the concentrated illumination.

**Keywords:** Cooling Cell; Dish-Style Concentration; Finite Element Method; Multijunction Solar Cell; Solar Radiation.

Kenza Djermane, Abdelhafid Habbab and Elhouaria Bourbaba:
Department of Science of Matter, The Semi-Conductor Device
Physics Laboratory, (LPDS) Bechar University, P.O.B no 417, Bechar
08000, Algeria, E-mail: djermane.kenza@yahoo.com (K. Djermane);
habbababdelhafid@gmail.com (A. Habbab); belhouaria@yahoo.fr
(E. Bourbaba)

#### 1 Introduction

III—V compound semiconductors are the most convenient materials to the manufacture of the high-efficiency solar cells for their high reliability, e.g. the wide range of solar spectrum conversion, the good ratio of the efficiency-weight, the excellent resistance to the solar radiation, and the low coefficient of voltage/temperature [1–3]. Among these materials, we can find InGaP, (In)GaAs, and Ge, which are the most suitable semiconductors for the concentrator photovoltaic (CPV) applications, as they have the highest efficiencies and the best response to the high temperatures.

The CPV technology can generate significant the energy. This is why it is mainly adapted for the high-energy plants to compete with the conventional fossil fuel plants [4, 5]. In a concentrator system, we can notice a small area of the efficient, but very expensive cell material is required at the focal point. The large collecting area is replaced by the cheap concentrator optics that results in a significant decrease in the system cost. It should be noted that the concentration level also has an important influence on the cost. The solar cell cost greatly decreases when a higher concentration ratio is used. This makes the high-efficiency cells more economic, although the concentration concept is old, while the CPV technology is still considered new [1].

The concentrated photovoltaic systems have been widely investigated for aiming and improving the cost-efficiency balance in the solar energy field. An important issue is given by the cell cooling. As the cell efficiency and stability typically were decreasing with the temperature, solar cells were performed better at the low temperatures. Modelling the performance of the multifunction solar cells as a function of temperature and concentrated radiation has been well presented in the literature [6–9]. The modelling of a single diode is used by several authors to deduce the different parameters of the subcells [10–12].

In this article, the objective is to determine the subcells limit temperature that requires a cooling system in the arid and semiarid regions. For this, we have studied the effect of the temperature and concentrated illumination on the performance of the individual top at the middle

<sup>\*</sup>Corresponding author: Syham Kadri, Department of Science of Matter, The Semi-Conductor Device Physics Laboratory, (LPDS) Bechar University, P.O.B no 417, Bechar 08000, Algeria, E-mail: syhammiss@yahoo.fr

and bottom subcells InGaP/InGaAs/Ge multijunction solar cell (MJSC). The results are shown that the bottom solar cell is very sensitive to the temperature and concentrated illumination.

## 2 Theoretical Approach

Figure 1 shows the physical problem studied. It consists of the InGaP/InGaAs/Ge MJSC under the high-concentrated illumination (parabolic dish system), and the In $_{0.5}$ Ga $_{0.5}$ P/In $_{0.01}$ Ga $_{0.99}$ As/Ge triple junction solar cell structure displays detailed layers with all parameters including doping concentration. The solar cell structure consists of an InGaP top cell, an InGaAs middle cell, and a Ge bottom cell. The InGaP top cell of a gap energy 1.85–1.9 eV absorbs the short part of the solar spectrum [13]. This cell is remaining transparent to the light of the longer wave length [14]. This light is absorbed more effectively by the (In)GaAs middle cell of the gap energy (1.41–1.435 eV) [15, 16]. The Ge bottom cell of the gap energy (0.65–0.67 eV) absorbs all the light [17]. The triple junction cells are series connected by two p<sup>++</sup>/n<sup>++</sup> tunnel junctions.

Table 1 summarises the parameters used in our simulation at  $T=300\,\mathrm{K}$  [18]. These parameters are influenced by the temperature. The mobility of the electrons and holes is decreased significantly with the temperature, and several experimental studies have given the descriptive relationships of this variation [19–21]. Also, the effective states density of the electrons and holes increases slightly with the temperature by a proportionality of  $T^{3/2}$ . The band gap energy is therefore a function of lattice temperature, following the Varshni relationship [22]:

$$E_g = E_g(0) - \frac{\alpha T^2}{T + \beta} \tag{1}$$

where the  $E_g(0)$  is the band gap at 0 K;  $\alpha$  and  $\beta$  are constants given in Table 1. Given the effect of the material composition that allows the model to handle different types of cells. For the semiconductor alloys, the band gap can be determined by the following relation [4]:

$$E_g(A_{1-x}B_x) = xE_g(B) + (1-x)E_g(A) + x(1-x)P$$
 (2)

 $A_{1-x}$  and  $B_x$  composition of alloy and P factor depend on alloy to include variations from the linear function.

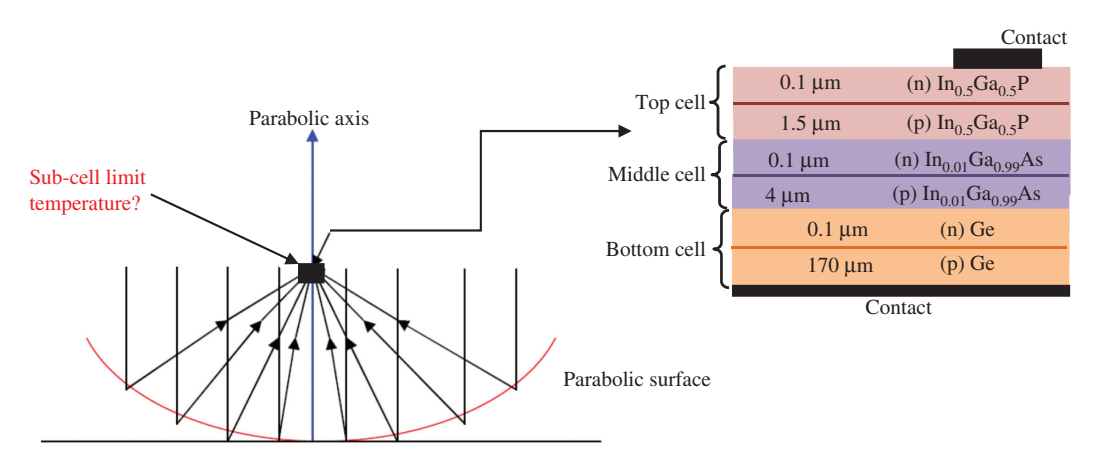


Figure 1: Physical model.

Table 1: The major parameters for InGaP, InGaAs, and Ge at 300 K [18].

Parameters	Top cell InGaP	Middle cell InGaAs	Bottom cell Ge	
Lattice constant (A°)	5.65	5.65	5.66	
Band gap (eV)	1.86	1.41	0.67	
Mobility of hole (cm²/V⋅s)	1000	400	1900	
Mobility of electron (cm <sup>2</sup> /V⋅s)	4000	8000	3900	
Permittivity	11.75	13.1	16	
Effective density of states in the conduction band Nc (cm $^{-3}$ )	$1.3\times10^{20}$	$4.7  imes 10^{17}$	$1.04\times10^{19}$	
Effective density of states in the valence band Nv ( $cm^{-3}$ )	$\boldsymbol{1.2\times10^{19}}$	$9  imes 10^{18}$	$6\times10^{18}$	
Affinity $\chi$ (eV)	4.08	4.07	4	
$N_D \text{ (cm}^{-3})$	$3 \times 10^{18}$	$5 imes10^{18}$	$1 \times 10^{19}$	
$N_A \text{ (cm}^{-3})$	$5  imes 10^{17}$	$5  imes 10^{17}$	$2\times10^{17}$	
$E_a(0)$ (eV)	1.915	1.5216	0.742	
$\alpha$ (eV/K)	$3.1 \times 10^{-4}$	$5.41 \times 10^{-4}$	$4.81 \times 10^{-4}$	
β (K)	248	204	235	

If the subcells of the solar cell are composed of alloys, then (1) will be adapted to accurately model the dependence of the temperature on the band gap. It is worth to mention that earlier numerical models did not take into account the alloy composition band gap in consideration.

Figure 2 represents the single-diode model circuit for the MJSC. The triple-junction solar cell consists of three junctions linked in series. Every junction was expressed by the single-diode model. The J–V relation of the subcells is given by [11, 23]:

$$J = J_{\text{ph},i} - J_{0,i} \left( e^{\frac{q(V_i + JR_{s,i})}{nk_B T}} - 1 \right) - \frac{(V_i + JR_{s,i})}{R_{\text{sh},i}}$$
(3)

where i represents the number of subcells (1 = top, 2 = middle, and 3 = bottom), J is the current density, V is the voltage,  $J_{\rm ph}$  is the photogenerated current density,  $J_0$  is the diode saturation current density,  $k_B$  is the Boltzmann's constant, T is the temperature, n is ideality factor,  $R_s$  is series resistance, and  $R_{\rm sh}$  is shunt resistance.

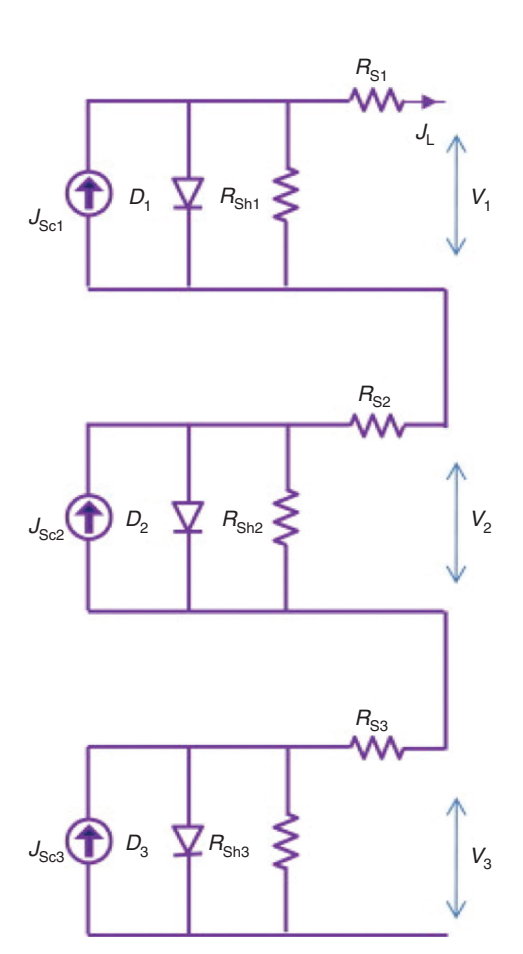


**Figure 2:** The single-diode model circuit for the multijunction solar cell.

From this model, we can deduce the short-circuit current density ( $J_{sc}$ ), the open-circuit voltage ( $V_{oc}$ ), the fill factor (FF), and the conversion efficiency ( $\eta$ ) by the following formulas [11, 23]:

$$J_{\rm sc} \approx J_{\rm ph}$$
 (4)

$$V_{\rm oc} = \frac{k_B T}{q} \ln \left( \frac{J_{\rm sc}}{J_0} + 1 \right) \tag{5}$$

$$FF = \frac{P_{\text{max}}}{J_{\text{sc}} \cdot V_{\text{oc}}} \tag{6}$$

$$\eta = \frac{P_{\text{max}}}{P_{\text{in}}} \tag{7}$$

where  $P_{\text{max}}$  is the maximum power that was delivered by the cell, and  $P_{\text{in}}$  is the incident light power.

### 2.1 Temperature Under Concentration

When the MJSC is subjected to a high concentration (1000 sun), the heat can be dissipated. This heat can cause highly problematic for the MJSC performance under the concentration. It will increase the operating temperature of the device if an appropriate thermal paste is not used between the cell and the carrier [17, 24]. As temperature is increasing, the most significant effect on semiconductors is decreased in the band gap of the material (1), which implies an increase in the photocurrent. The performance of the MJSC is influenced by the temperature under concentration as follows:

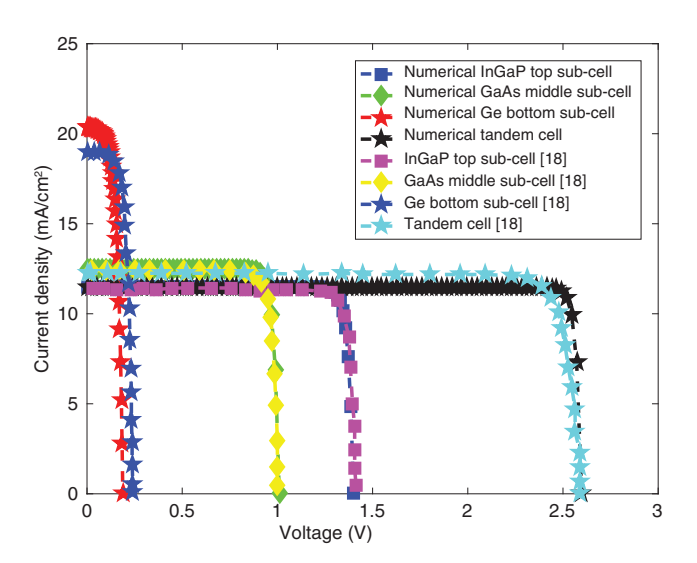


Figure 3: Validation of J-V characteristics of the individual top, middle, and bottom subcells of InGaP/InGaAs/Ge solar cell.

The temperature has a very negligible impact on the MJSC short-circuit current density ( $J_{sc}$ ) as a function of concentration by the following approximation [25]:

$$J_{\rm sc}(T, X {\rm sun}) = X J_{\rm sc}(T, 1 {\rm sun}) \tag{8}$$

The open-circuit voltage as a function of concentration is much influenced by the temperature. The slope of  $V_{\rm oc}$  as a function of concentration increases for increasing

the temperature due to the following equation [18]:

$$V_{\rm oc}(X,T) = V_{\rm oc}(T,1\sin) + \frac{nKT}{q}ln(X)$$
 (9)

Among the parameters most influenced by the temperature is the temperature coefficient  $V_{\text{oc}}$  that was studied theoretically [26, 27] as well as experimentally [28–31].

**Table 2:** Performance parameters of simulated multijunction cell compared with model data.

	$J_{\rm sc}$ (mA/cm <sup>2</sup> )	V <sub>oc</sub> (V)	P <sub>max</sub> (mW)	FF	η (%)
InGaP top subcell	11.46	1.40	14.5845	0.9090	14.585
	11.43	1.41	14.3328	0.889	14.333
GaAs middle subcell	12.50	1.01	11.1255	0.8812	11.126
	12.41	1	10.7867	0.869	10.787
Ge bottom subcell	20.35	0.188	2.4035	0.6282	2.4035
	18.96	0.24	3.1330	0.6885	3.1330
Tandem cell	11.46	2.598	28.0920	0.9435	28.092
	11.43	2.59	27.7394	0.937	27.739

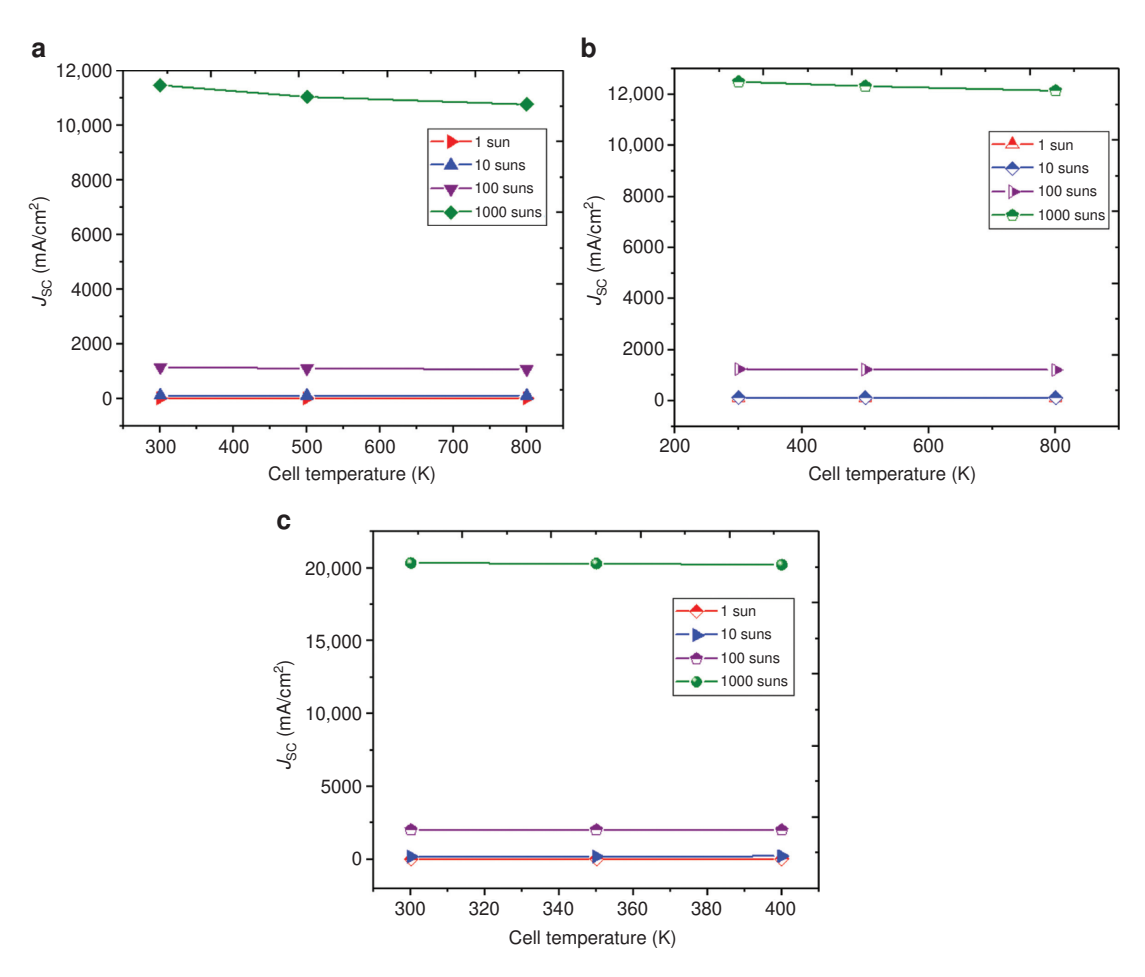


Figure 4: Effect of temperature and concentrated sunlight on short-circuit current density  $J_{sc}$  for top subcell (a), middle subcell (b), and bottom subcell (c).

The  $\eta$  and the *FF* are involved with the temperature. They decrease with increasing temperature [18].

$$\eta = \frac{P_{\text{max}}}{P_i} = \frac{J_{\text{max}}.V_{\text{max}}}{X.P_{\text{inc}}} \tag{10}$$

## 3 Numerical Approach

In order to achieve our objective, we have solved the system of partial differential equations consisting of J–V relation (3); the drift-diffusion model, which consists of the continuity equations [(11) and (12)]; and current density equations for electrons and holes [(13) and (14)], respectively, coupled with Poisson's equation (15) with appropriate boundary conditions, using the Galerkin finite element method. The one-dimensional spatial domain is divided into 521 elements.

Temporal continuity equations for electrons and holes are as follows [32, 33]:

$$\frac{\mathrm{d}n}{\mathrm{d}t} = \frac{1}{q} \frac{\mathrm{d}J_n}{\mathrm{d}x} + R_n - G \tag{11}$$

$$\frac{\mathrm{d}p}{\mathrm{d}t} = \frac{1}{q} \frac{\mathrm{d}J_p}{\mathrm{d}x} + R_p - G \tag{12}$$

where t is the time; x is the position; n and p are the concentration density of electrons and holes, respectively;  $R_n$  and  $R_p$  are the recombination rate of electrons and holes, respectively; q is the charge element; and G is the optical carrier generation rate.  $J_n$  and  $J_p$  represent the current densities of electrons and holes, respectively, and can be written as follows [34, 35]:

$$\overrightarrow{J_n} = qn\mu_n \vec{E} + qD_n \vec{\nabla} n \tag{13}$$

$$\overrightarrow{J_p} = qp\mu_p \vec{E} - qD_p \vec{\nabla} p \tag{14}$$

The Poisson's equation is as follows [36–39]:

$$\frac{\partial^2 \phi}{\partial x^2} = -\frac{\mathrm{d}E}{\mathrm{d}x} = -\frac{q(n-p+N_D-N_A)}{\varepsilon} \tag{15}$$

For (13), (14), and (15), we find  $\mu_n$  and  $\mu_p$  are the charge carrier mobility for electrons and holes, respectively,  $\varepsilon$  is

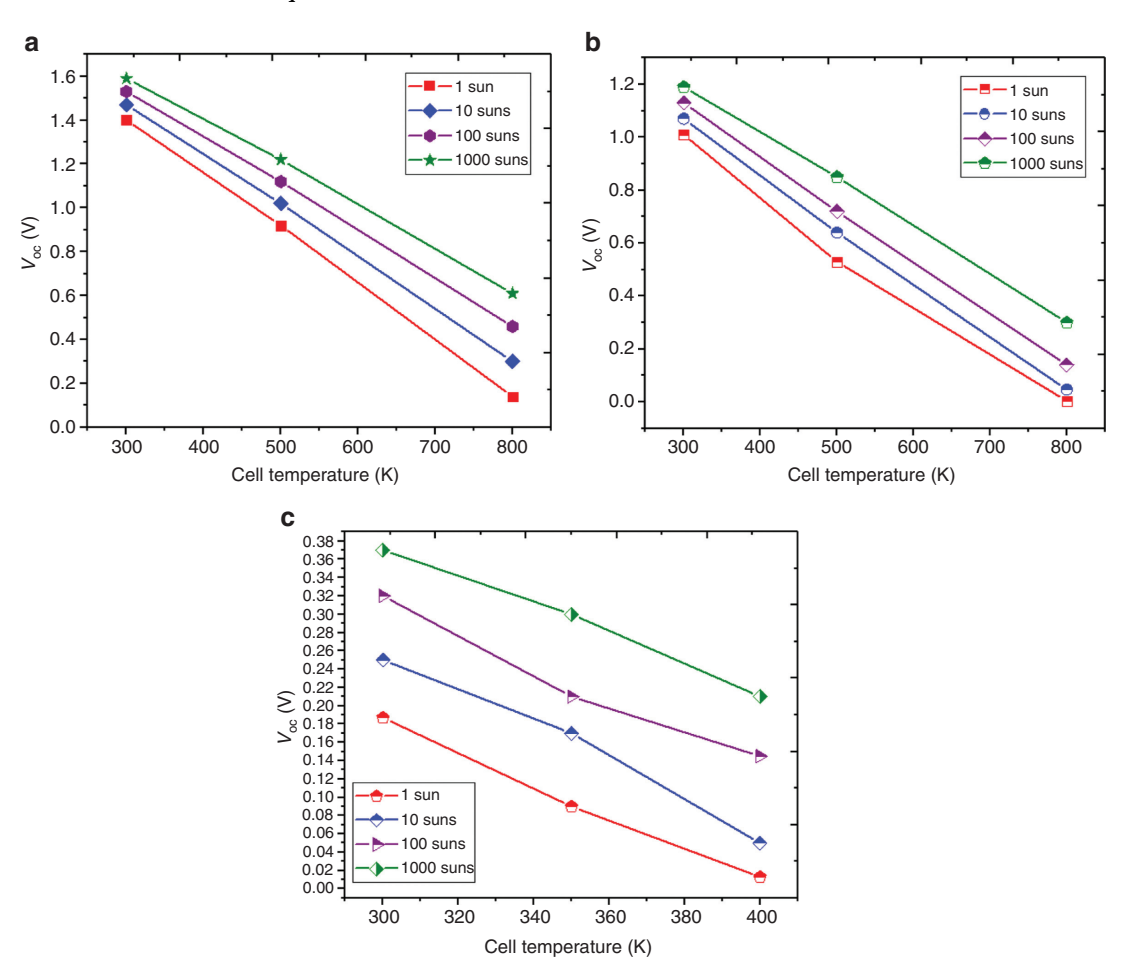


Figure 5: Effect of temperature and concentrated sunlight on open-circuit voltage  $V_{oc}$  for top subcell (a), middle subcell (b), and bottom subcell (c).

the semiconductor permittivity ( $\varepsilon = \varepsilon_0 \varepsilon_r$ );  $\phi$  is the local electric potential;  $N_D$  and  $N_A$  are the donor and acceptor concentrations, respectively; and  $D_n$  and  $D_p$  are diffusion constants for electron and holes, respectively, which are given by the following [40]:

$$D_n = \frac{k_B T}{q} \mu_n \tag{16}$$

$$D_p = \frac{k_B T}{q} \mu_p \tag{17}$$

This article adopts the detailed balance principle, which is summarised concisely as follows. First, the generation introduced into the continuity equations (11) and (12) is due to sunlight. This process is known as an optical generation. Second, the recombination current is dictated strictly according to Schokley–Read–Hall (SRH) trap recombination. This process depends mainly on the density of the deep levels and therefore the quality of the

material. The SRH recombination is expressed by [41]:

$$R_{\text{SRH}} = \frac{pn - n_i^2}{\tau_{p0} \left[ n + n_i \exp\left(\frac{E_t - E_i}{k_B T_L}\right) \right] + \tau_{n0} \left[ p + n_i \exp\left(\frac{E_i - E_t}{k_B T_L}\right) \right]}$$
(18)

where  $E_t$  is the trap states energetic position;  $E_i$  is the Fermi level in the intrinsic semiconductor;  $\tau_{n0}/\tau_{p0}$  are the lifetime for the electrons and the holes, respectively;  $n_i$  is the intrinsic concentration;  $k_B$  is the Boltzmann constant; and  $T_L$  is the temperature in Kelvin.

### 4 Results and Discussion

To validate our results, we compared them with those of Walker [18]. The results in Figure 3 show an agreement between our numerical results and literature. Table 2

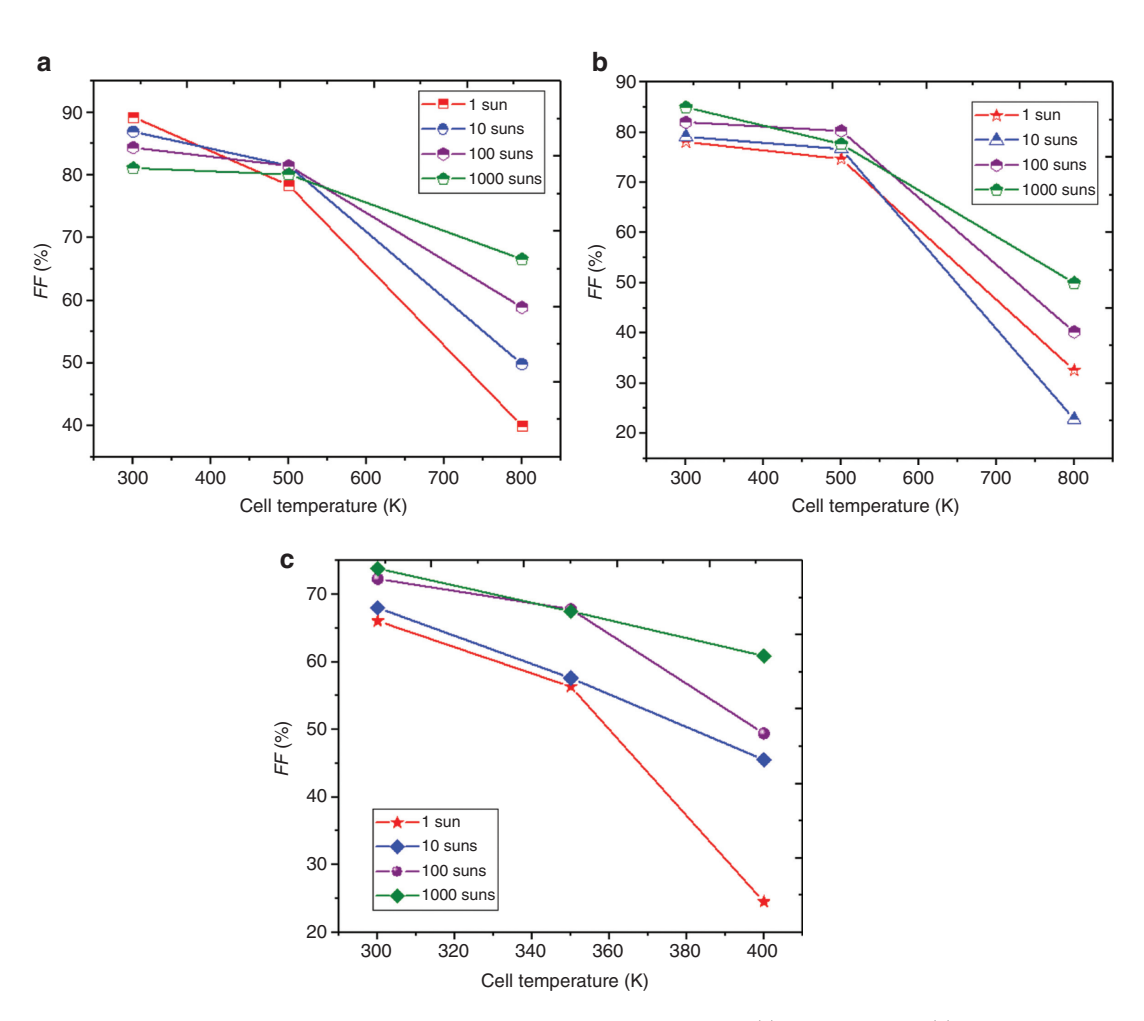


Figure 6: Effect of temperature and concentrated sunlight on FF for top subcell (a), middle subcell (b), and bottom subcell (c).

includes our numerical results (in blue) and those of Walker (in red) and confirms the observations made above.

In order to find the subcells limit temperature, we have exposed them to concentrated illumination between 1 and 1000 sun, and three temperature values are considered T=300,500, and 800 K. The choice of this temperature range is related to the type of concentrator chosen. We have presented the performance of each subcell as a function of temperature at different concentration ratios. The temperature limit is deduced when the open-circuit voltage goes to zero.

Figure 4 shows the short-circuit current density as a function of temperature and concentration for the three subcells. The effect of the concentrated radiation is more important on the short-circuit density compared to the effect of temperature.

Figure 5 illustrates the open-circuit voltage as a function of temperature and concentration for the three subcells. We observe that  $V_{\rm oc}$  increases linearly with

solar radiation and decreases with temperature. For concentration ratios of 1 and 10 sun,  $V_{\rm oc}$  disappears in the range of the temperature studied. The slope of  $V_{\rm oc}(T)$  shows that for the bottom subcells the amplitude of  $({\rm d}V_{\rm oc}/{\rm d}T)$  decreases visibly with the increase in the concentration ratio. For the Ge subcell, the decreasing of the open-circuit voltage approaches zero and leads to a collapse of the current-voltage (I–V) curves for temperatures greater than 400 K, which is why the temperature values for this cell are T=300,350, and 400 K. Opposed to this, data from the top and middle subcells indicate that its temperature sensitivity is increasing as the concentration ratio increases.

Figure 6 presents the *FF* dependence of the temperature on different values of concentration ratios for the three subcells. For all subcells, the *FF* increases until it reaches a maximum value, and then the behaviour reverses. For the top and middle subcells, this maximum value is deduced at temperature about 500 K. For

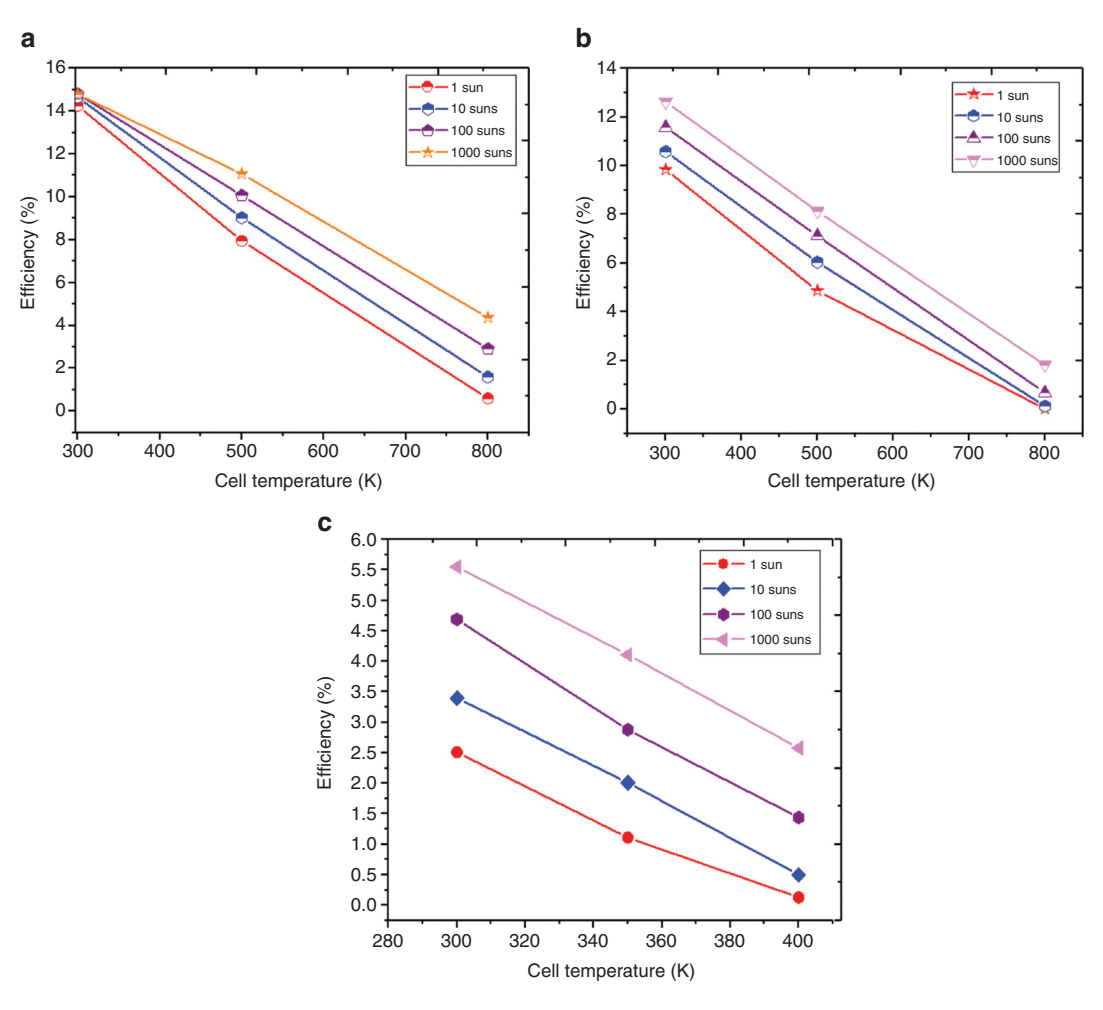


Figure 7: Effect of temperature and concentrated sunlight on efficiency conversion  $\eta$  for top subcell (a), middle subcell (b), and bottom subcell (c).

the bottom subcell, the temperature value is 350 K. This behaviour is due to the sharp drop in the open-circuit voltage.

The variation of the  $\eta$  as a function of the temperature at different concentration ratios for the three subcells is shown in Figure 7. The  $\eta$  decreases with increasing temperature and increases as a function of the concentrated radiation. This increase is controlled by the logarithmic increase of  $V_{\rm oc}$  with intensity. However, as the concentration increases, this effect is compromised by the reduction of *FF* cells due to losses of resistance in series.

### 5 Conclusion

A cooling temperature for InGaP/InGaAs/Ge subcells under concentration is developed and introduced in this study. The single-diode model of the equivalent circuit for subcells multijunctions and the drift-diffusion model coupled with the Poisson equation have been used successfully. The three subcells paired in Ga<sub>0.50</sub>In<sub>0.50</sub>P, In<sub>0.01</sub>Ga<sub>0.99</sub>As, and Ge were studied over a wide range of temperature and irradiance. The top Ga<sub>0.50</sub>In<sub>0.50</sub>P subcell and the middle subcell Ga<sub>0.99</sub>In<sub>0.01</sub>As are almost in paired current across the entire temperature range. As the temperature increases, a change from a slight limitation of the top and middle subcells is observed. The decrease in short-circuit density as a function of temperature is low compared to the bottom cell, which is invisible. The results of the open-circuit voltage for the three subcells show that at high temperature, for the Ge subcell, the decrease of the open-circuit voltage approaches zero and leads to a collapse of the I-V curve for temperatures greater than 400 K. For the three subcells and at different concentrations. The FF and  $\eta$  decrease with temperature. Finally, we can conclude that the limit temperature is equal to 400 K, because the cooling system is necessary and will be placed in parallel with our CPV system in order to avoid the degradation of InGaP/InGaAs/Ge MJSC.

### References

- A. Mahfoud, Modeling Thin-Film Tandem Solar Cells With High Efficiency, PhD Thesis, Université Setif 1, Setif, Algeria 2015.
- [2] T. Markvart and L. Castaner, Practical Handbook Photovoltaics: Fundamentals and Applications, 2<sup>nd</sup> edition, Elsevier, Amsterdam, The Netherlands 2003, ISBN:1856173909.
- [3] F. Dimorth and S. Kartz, Adv. Inorg. Mater. Photovoltaics 32, 230 (2007).
- [4] I. Vurgaftman, J. R. Meyer, and L. R. Ram-Mohan, J. Appl. Phys. 89, 5815 (2001).

- [5] A. Ghoneim, K. M. Kandil, T. H. Alzanki, and M. R. Alenezi, Int. J. Sustain. Energ. 37, 294 (2017).
- [6] F. Newman, D. Aiken, P. Patel, D. Chumney, I. Aeby, et al., in: 34th IEEE Photovoltaic Specialists Conf. (PVSC), Philadelphia, PA 2009, p. 1611.
- [7] T. Marios, E. F. Fernández, C. Stark, T. S. O'Donovan, Energ. Convers. Manage. 117, 218 (2016).
- [8] R. Olivier, A. Jaouad, B. Bouzazi, R. Arès, S. Fafard, et al., Sol. Energ. Mat. Sol. C. 144, 173 (2016).
- [9] V. S. Kalinovsky, E. V. Kontrosh, P. A. Dmitriev, P. V. Pokrovsky, A. V. Chekalin, et al., AIP Conf. Proc. 1616, 8 (2014).
- [10] A. Kribus and G. Mittelman, in: Proceedings of the International Conference on Concentrated Solar Concentrators for the Generation of Electricity or Hydrogen (ICSC-4), Spain 2007.
- [11] G. Segev, G. Mittelman, and A. Kribus, Sol. Energ. Mat. Sol. C. 98, 57 (2012).
- [12] A. Ben Or and J. Appelbaum, Prog. Photovoltaics Res. Appl. 21, 713 (2013).
- [13] R. M. Swanson, Prog. Photovoltaics Res. Appl. 8, 93 (2000).
- [14] F. Djaafar, B. Hadri, and G. Bachir, J. Electr. Syst. 14, 64 (2018)
- [15] F. Kürker, Micro Fabrication Based Design and Simulation of Heterojunction Solar Cell, Master's Thesis, Çukurova University Institute of Natural and Applied Sciences, Adana, Turkey 2010.
- [16] B. P. Sullivan, The Effect of Temperature on the Optimization of Photovoltaic Cells Using Silvaco Atlas Modelling, Master Thesis 2010.
- [17] K. P. O'Donnell and X. Chen, Appl. Phys. Lett. 58, 2924 (1991).
- [18] A. W. Walker, Bandgap Engineering of Multijunction Solar Cells Using Nanostructures for Enhance Performance Under Concentrated Illumination, PhD Thesis, Canada 2013.
- [19] D. Ahmari, M. Fresina, Q. Hartmann, P. Barlage, M. Feng, et al., IEEE Electr. Device L. 18, 559 (1997).
- [20] J. M. Olson, D. J. Friedman, and S. Kurtz, High Efficiency III-V Multijunction Solar Cells, John Wiley & Sons, Hoboken, NJ, USA 2003, ISBN:9781118755631.
- [21] M. R. Brozel and G. E. Stillman, Properties of Gallium Arsenides, 3<sup>rd</sup> edition, IEE/INSPEC, Institution of Electrical Engineers, Piscataway, NJ, USA 1996.
- [22] Y. Varshni, Physica 34, 149 (1967).
- [23] K. C. Reinhardt, Y. K. Yeo, and R. L. Hengehold, J. Appl. Phys. 77, 5747 (1995).
- [24] J. F. Wheeldon, A. Walker, C. E. Valdivia, S. Chow, O. Theriault, et al., AIP Conf. Proc. 1407, 220 (2011).
- [25] J. Nelson, The Physics of Solar Cells, Imperial College Press, London, UK 2003.
- [26] A. Ben Or, P. Fuss-Kailuweit, S. P. Philipps, U. Fiedeler, S. Essig, et al., in: Conference Proceeding From the 27th European Photovoltaic Solar Energy Conference and Exhibition, Frankfurt, Germany, September 24–28, 2012, p. 150.
- [27] A. W. Walker, J. F. Wheeldon, O. Theriault, M. D. Yandt, and K. Hinzer, in: Proceeding From the 37th IEEE Photovoltaic Specialist Conference (PVSC-37), Seattle, WA 2011.
- [28] J. F. Geisz, A. Duda, R. M. France, D. J. Friedman, I. Garcia, et al., AIP Conf. Proc. 1477, 44 (2012).
- [29] G. S. Kinsey, P. Hebert, K. E. Barbour, D. D. Krut, H. L. Cotal, et al., Prog. Photovoltaics Res. Appl. 16, 503 (2008).

- [30] K. Nishioka, T. Sueto, M. Uchida, and Y. Ota, J. Electron. Mater. 39, 704 (2010).
- [31] G. A. Landis, D. Belgiovane, and D. Scheiman, in: Proceeding of the 37th IEEE Photovoltaic Specialist Conference (PVSC), Seattle, WA 2011.
- [32] H. Mathieu, Physique des semi-conducteurs et des composants électroniques, 4ème édition, Masson, Paris
- [33] M. Orgeret, Les piles solaires le composant et ses applications, Masson, Paris 1985.
- [34] ATLAS User's Manual: Device Simulation Software, SILVACO International, Santa Clara, CA 2012.
- [35] A. Adaine, Optimisation numérique de cellules solaires à très haut rendement à base d'InGaN, Université de Lorraine, France 2018.

- [36] J. Piprek, Semi-conductor Optoelectronic Devices: Introduction to Physics and Simulation, Academic Press, Waltham, MA 2013, ISBN:9780080469782.
- [37] J. S. Yuan and J. J. Liou, Semi-conductor Device Physics and Simulation, Springer, New York, NY, USA 1998, ISBN:978-1-4899-1904-5.
- [38] K. Nishioka, T. Takamoto, T. Agui, M. Kaneiwa, Y. Uraoka, et al., Jpn. J. Appl. Phys. 43, 882 (2004).
- [39] F. Lévy, Physique et technologie des semi-conducteurs. PPUR presses polytechniques, Lausanne, Switzerland 1995.
- [40] M. Joseph, Fundamentals of Semiconductor Physics, Anchor Academic Publishing, Hamburg, Germany 2015, ISBN:9783954899197.
- [41] B. Van Zeghbroeck, Principles of Semiconductor Devices, Prentice Hall, Upper Saddle River, NJ 2011.